Numerical Evaluation of Effective Gas Diffusivity – Saturation Dependence of Uncompressed and Compressed Gas Diffusion Media in PEFCs

V. P. Schulz[a], P. P. Mukherjee[b], J. Becker[a], A. Wiegmann[a], and C.-Y. Wang[b]

[a]Fraunhofer-ITWM, Kaiserslautern 67663, Germany
[b]Electrochemical Engine Center, Pennsylvania State University, University Park, Pennsylvania 16802, USA

In the current work, we present a comprehensive modeling framework to predict the effective gas diffusivity, as a function of liquid water saturation, based on realistic 3-D microstructures of the uncompressed as well as compressed gas diffusion layer (GDL). The presented approach combines the generation of a virtual microscopic GDL and different physical modeling. We develop a reduced model in order to simulate the compression of the GDL layer since its compression has a strong impact on the material properties such as the water transport or its gas diffusion. Then, we determine the two-phase distribution of a non-wetting fluid, i.e. water, and a wetting fluid, i.e. air, within the GDL for different saturations. This is done using a full morphology (FM) model. Finally, solving the Laplace equation for the partly saturated medium we determine the relative gas diffusion, i.e. the gas diffusion depending on the saturation. In the present work, our approach is applied to a typical GDL medium, a SGL10BA carbon paper.

Introduction

The gas diffusion layer (GDL) plays a crucial role in the overall water management of a polymer electrolyte fuel cell (PEFC), which requires a delicate balance between reactant transport from the gas channels and water removal from the electrochemically active sites (1). Till date, the prediction of the effective transport properties, such as the permeability, heat transport coefficient, and gas diffusivity, to be employed in the macroscopic fuel cell models is a challenge. This is especially true for saturation dependent parameters such as the relative permeability or the relative gas diffusion coefficient at high current density operation. Of paramount importance is the estimation of volume blockage effect due to liquid water within the GDL, rendering hindered oxygen transport to the active reaction sites.

Outline

In the current work, we present a comprehensive modeling framework to predict the effective gas diffusivity, as a function of liquid water saturation, based on realistic 3-D microstructures of the uncompressed as well as compressed GDL. Our approach includes four steps:

1. Reconstruction of the 3-D GDL microstructure;
2. Compression of the reconstructed 3-D digital structure under clamping pressure;
3. Determination of the 3-D liquid water saturation distributions depending on the capillary pressure, and
4. Determination of the gas diffusion coefficient for different liquid water saturation levels.

Microstructure Generation

In our approach, the construction of a realistic GDL pore morphology is the essential prerequisite for unveiling the influence of the underlying structure on the two-phase behavior. For a wide range of typical GDL media, such as carbon papers, their microscopic description is rather simple. They are built up from single fibers with a given diameter and the ensemble follows a stochastic distribution. Thus, a stochastic generation model is the method of choice for the microstructure generation due to the low cost and the high speed of the data generation. Nevertheless, a stochastic model for carbon papers can be very complicated if one includes the crimp of the fibers, for example. In order to develop a manageable model for the microstructure generation, the following assumptions are made about the investigated carbon-paper GDLs:

- The fibers are long compared to the sample size and their crimp is negligible
- The interaction between the fibers can be neglected, i.e. the fibers are allowed to overlap
- Due to the fabrication process, the fiber system is macroscopically homogeneous and isotropic in the material pane, defined as xy-plane

Details about our stochastic model can be found in (2). The reconstructed microstructure of t a SGL10BA, which has been used for further simulations, is shown in Fig. 1.

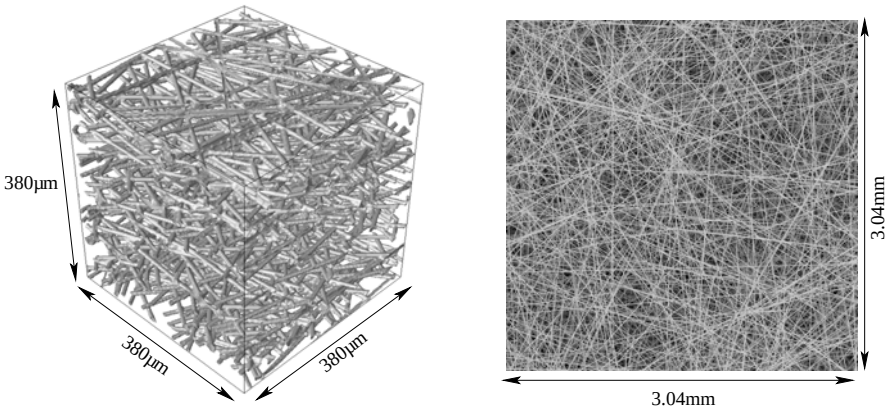

Figure 1. 3-D and 2-D visualizations of the generated microstructure based on the properties of a SGL10BA carbon paper. The 2-D image is a visualization looking from the top on the image similar to a SEM.

Microstructural characterization

The structural properties, namely, the pore size distribution and the intrinsic permeability of the GDL microstructure are evaluated in order to validate the digital model against the physical properties of the real carbon paper GDL. The pore size distribution is determined by a morphological opening with spheres, similar as the concept of granulometry. The determined pore radii range from 1.5 to 40 μm with a maximum between 12 and 20 μm. The lower limit for the pore radius in our simulation is given by the image resolution which is 1.48 μm/voxel.

A comparison between the simulated permeability and measured data is shown in Table I. The simulated in-plane permeability of the microstructure agrees very well with the measured data. For the through-plane permeability, the results are still acceptable since the deviation from the measured data is in the order of a macroscopic heterogeneity of the material. Additionally, the mismatch between our simulation and the measured data for the in-plane to through-plane permeability ratio of about 20% might be due to the larger anisotropy of the real SGL10BA compared to our reconstruction. This could be a consequence of the crimp of the fiber which has been neglected in our stochastic model.

TABLE I. Permeabilites of the generated microstructure as determined by a Lattice-Boltzmann flow simulation compared to measure data. Sample size is 512x512x256 voxel, i.d. 0.64 x 0.64 x 0.38 mm, respectively.

In-plane	**In-plane**	**Through-plane**	**In-plane/ Through-plane**
Simulation	30.9 darcy	21.1 darcy	1.46
Measured data (3)	33 darcy	18 darcy	1.83

Compression modeling

The detailed modeling of a porous material under compression is a challenging task of applied structural mechanics. In the context of the current work, a reduced model of compression is employed. The present model is based on a macroscopically homogeneous material which is fixed at one end (bottom) and loaded on the opposite end (top). Thus, the displacement is zero at the bottom and maximal at the top of the sample. Neglecting the transverse strain, we can transfer directly that macroscopic behavior into a displacement of the solid voxels. The compression ratio, c, is defined as:

$$c = \text{Height of the compressed sample/Initial height} \quad [1]$$

The new height, h', of each voxel can be calculated as its position along the z-axis by

$$h' = [c*h] \quad [2]$$

where h is the uncompressed position and the square brackets indicates rounding to the closest integer. Additionally, in our reduced compression model, we do not allow the solid voxels to penetrate into each other. Thus, with increasing compaction ratio more voxels lay on top of each other since the x-y-position is maintained fixed. However, with our reduced model, it is difficult to find a relation between the compression ratio and the external load. Nevertheless, due to the high porosity of the GDL material, our approach leads to a reliable 3-D morphology of the non-woven structures under compression as one can see from Fig. 2.

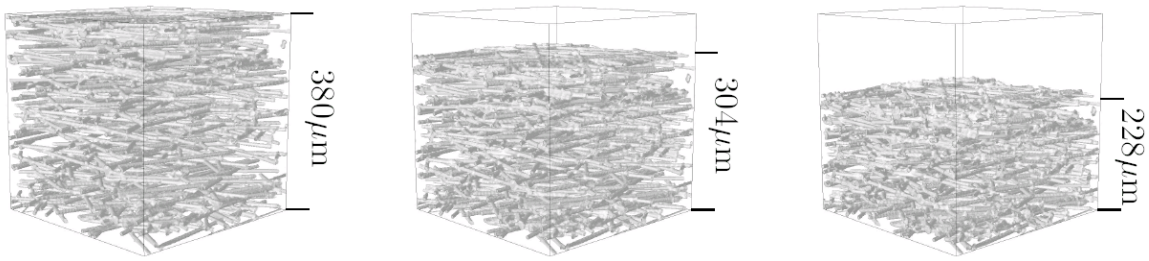

Figure 2. Visualization of the virtually compressed microstructure. From the left to the right, the compression ratios are 1.0, 0.8, and 0.6, respectively.

Simulation of the two-phase distributions

Once the three-dimensional microstructure of the gas diffusion medium is generated, the stationary distribution of the wetting and the non-wetting phases for arbitrary capillary pressure can be evaluated using a so-called full-morphology (FM) model. Details of this approach can be found in (4,5,6). The FM model can be used either to determine the two-phase distribution of a drainage process or in the case of repeated cycles of drainage and imbibiton. In the present work, we use the latter case since we are interested in the determination of an average phase distribution which can be seen as an 'intrinsic' capillary pressure-saturation function independent of special boundary condition. Therefore, we use the FM model in order to determine the arbitrary pore space where the capillary forces are small enough to be filled by the non-wetting phase fluid. A typical configuration is shown in Fig. 3.

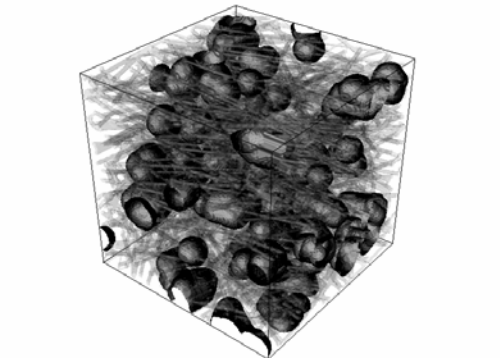

Figure 3. Simulated water distribution in the uncompressed microstructure as a result of the morphological opening. Shown is the configuration at a saturation of 17.5%.

Additionally, since the accessible pore space for the non-wetting phase consists of overlapping spheres with a given radius, r, we can estimate the according capillary pressure, p_c, by

$$p_c = 2\gamma/r * \cos\theta \qquad [3]$$

where γ is the surface tension between the non-wetting and the wetting phase and θ the contact angle between the wetting phase and the solid.

Consequentially, the FM model can be used for the uncompressed and the compressed microstructure. Three of the determined capillary pressure curves are shown in Fig. 4.

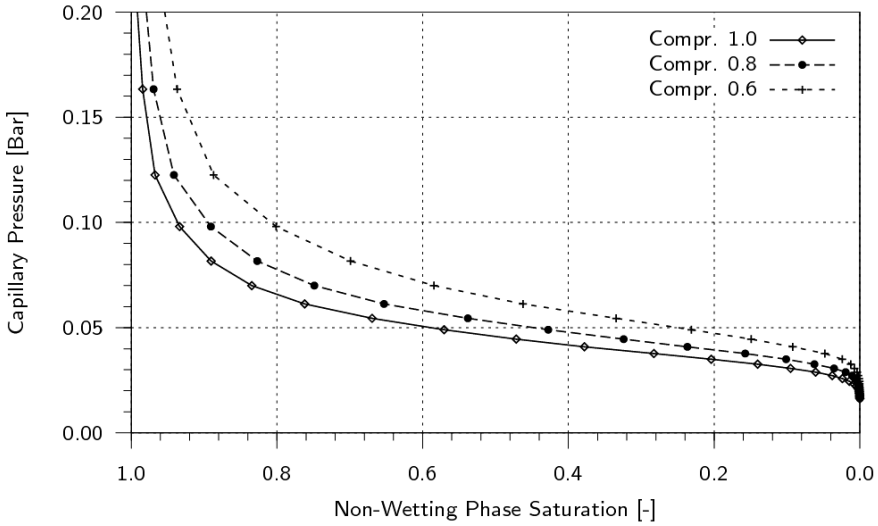

Fig. 4 Capillary pressure-saturation curves for the uncompressed and two different compression ratios. The underlying two-phase distribution corresponds to several drainage and imbibition cycles. For the calculation of the capillary pressure we assumed a contact angle of 120°.

Determination of the effective diffusion coefficient

Similar to the determination of the intrinsic permeability, one can calculate the diffusion coefficient of a porous medium based on the 3-D microstructure (7). This requires solving the Laplace equation

$$\Delta c = 0 \qquad [4]$$

for the concentration, c, with appropriate boundary conditions. The boundary conditions we use is a concentration gradient from the bottom to the top of the sample and no-flux conditions ($\partial c/\partial n=0$) in the solid and the wetting phase. Thus, the effective diffusion coefficient, D_{eff}, is derived by an integration over the 'field lines' in the volume:

$$D_{eff} = 1/V * \int \text{grad } c \, dV \qquad [5]$$

Note that the effective diffusion coefficient depends only on the pore space. Thus, without a porous medium, the effective diffusion coefficient is 1. This becomes more clear when relating D_{eff} to the tortuosity, τ, of the material by

$$D_{eff} = \Phi/\tau^2 \qquad [6]$$

where Φ is the porosity (8).

In our case, we determined a value of 0.74 for the effective diffusion coefficient of the uncompressed sample which is entirely filled by a gas phase. Since the porosity is 0.88, this corresponds to a tortuosity of 1.09 which is still close to one as expected from the 3-D microstructure shown in Fig. 1.

Using the previous steps of our approach, we study the dependency of the diffusion coefficient on the non-wetting phase saturation and the compression ratio where the results are shown in Fig. 5. Interestingly, the compression of the medium has the strongest impact on the diffusion coefficient for zero non-wetting phase saturation. This value is reduced from 0.74 in the uncompressed state to 0.61 for a compression ratio of 0.6. Interestingly, with increasing amount of the non-wetting phase saturation the effective diffusion coefficient becomes independent of the compression ratio.

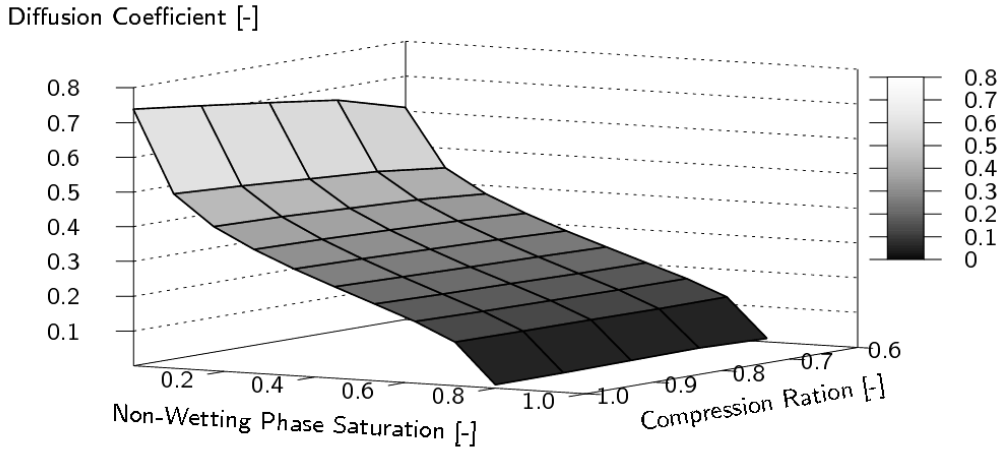

Fig 5. Dependency of the diffusion coefficient on the saturation and on the ratio of compression.

Conclusion

To our knowledge, this is the first presentation of a complete framework for the determination of capillary pressure-saturation curves and effective diffusion coefficients of a GDL under compression. The comprehensive modeling capability described in the present work is of significant importance in the determination of reliable input parameters for macroscopic simulations of the fuel cell. Our approach is also useful in terms of a virtual material design and optimization of the GDL due to the use of reduced physical models and due to recent advances in the numerical solution of elliptic partial differential equations in three-dimensional virtual microstructures (9).

Acknowledgments

We acknowledge financial support for this work from the BMBF-project PEMDesign (03SF0310A) and from the Kaiserslautern Excellence Cluster Dependable Adaptive Systems and Mathematical Modelling.

REFERENCES

1. M. Mathias, J. Roth, J. Fleming, and W. Lehnert, in: *Handbook of Fuel Cells Volume 3*, W. Vielstich, A. Lamm, and H. Gasteiger, Editors, p. 1, John Wiley & Sons Ltd., New York (2003)
2. K. Schladitz, S. Peters, D. Reinel-Bitzer, A. Wiegmann, and J. Ohser, accepted in *Computational Materials Science*, doi:10.1016/j.commatsci.2006.01.018
3. J. Ihonen, M. Mikkola, and G. Lindbergh, *J. Electrochem. Soc.*, **151**, A1152 (2004)
4. M. Hilpert and C. T. Miller, *Adv. Water Resour.*, **24**, 243 (2001)
5. H.-J. Vogel, J. Tölke, V. P. Schulz, M. Krafczyk, and K. Roth, *Vadose Zone Journal*, **4**, 380 (2005)
6. V. P. Schulz, P. P. Mukherjee, J. Becker, A. Wiegmann, and C.-Y. Wang, submitted to *J. Electrochem. Soc.*
7. V. Schulz, D. Kehrwald, A. Wiegmann, and K. Steiner, *Proceedings of 2nd NAFEMS CFD-Seminar: Flows (CFD) - Application and Trends*, p. 6.1, Niedernhausen, Germany (2005).
8. N. Epstein, *Chem. Eng. Science,* **44**, 3 (1989)
9. http://www.geodict.com